Electronic structure of halogen-substituted methyl radicals: Excited states of CH_2Cl and CH_2F

Sergey V. Levchenko and Anna I. Krylov
Department of Chemistry, University of Southern California, Los Angeles, California 90089-0482

(Received 21 May 2001; accepted 16 July 2001)

Electronically excited states in CH_2Cl and CH_2F radicals are studied at the EOM–CCSD/6-311(3+, 3+)G(3df, 3pd) level of theory. Excited states' characters and changes in the electronic spectrum in the $CH_3 \rightarrow CH_2F \rightarrow CH_2Cl$ sequence are interpreted in terms of a simple molecular orbital picture. The key factors determining the electronic structure of these radicals are (i) the presence of lone pairs on the halogen and (ii) how strongly these lone pairs are bound to the halogen. In CH_2Cl, the small energy gap between the unpaired electron on carbon and the lone pair on chlorine results in additional π-bonding between C and Cl. Moreover, the relatively weak binding energy of the chlorine's lone pairs is responsible for the presence of several low-lying valence states in CH_2Cl. In CH_2F, where the lone pairs have a considerably lower energy, no additional bonding is found. The character of two lowest valence states in CH_2F is similar to that of the lowest states in CH_2Cl, but the excitation energies are considerably higher. The low-lying Rydberg states appear to be similar in all three radicals. © *2001 American Institute of Physics.* [DOI: 10.1063/1.1400143]

I. INTRODUCTION

Halogen-substituted methyl radicals are intermediates in the photodecomposition and oxidation reactions of halogenated hydrocarbons which represent an important source of halogen atoms in the atmosphere.[1,2] Since atmospheric reactions occur at relatively low concentrations, and in the presence of solar radiation, the photodissociation of these radicals may compete with nonphotochemical pathways of their decomposition, e.g., bimolecular reactions with other species.

It has been revealed by earlier spectroscopic (see Ref. 3 for the summary of spectroscopic data) and *ab initio*[4] studies that the seeming similarity between the methyl radical and its halogen-substituted derivatives is limited and even deceptive: the interaction of the lone pairs of halogen(s) with the unpaired electron is the cause of anomalously strong C-halogen bonds,[5–9] deviations from planarity,[5,6] and high anharmonicity of the out-of-plane vibrations.[7,8] Moreover, the availability of nonbonding electrons suggests the presence of low-lying valence excited states in halogenated methyl radicals, as opposed to the methyl radical whose lowest electronically excited states are almost exclusively Rydberg states.[10–14]

Experimental studies of the excited states in halogenated methyl radicals are scarce.[15–21] Several Rydberg states of CH_2F have been probed by resonance enhanced multiphoton ionization (REMPI) spectroscopy by Hudgens *et al.*[15] Rousel *et al.* have measured the ultraviolet absorption spectrum of CH_2Cl in the 195–235 nm range.[18] Recently, the photodissociation dynamics of CH_2Cl has been studied by the photofragment imaging technique by Reisler and co-workers.[22] They have also employed the REMPI technique to probe Rydberg states.[22] Earlier, estimations of the energies of the lowest excited state in CH_2Cl and CH_2F have been derived from analysis of microwave spectra.[23]

Theoretical studies of excited states in these species[15–17,24–27] have been mostly limited to a selected subset of states such as excited states different in symmetry from the ground state[15–17,24–26] (calculated by Hartree–Fock and MP2). The Rydberg states of these radicals have been indirectly studied by calculating the corresponding ground state cations.[24–26,28] Recently, Li and Francisco have reported multireference configuration interaction (MRCI) calculations of several valence states of CH_2Cl and CH_2Br.[27]

The goal of the present study is to accurately investigate *both valence and Rydberg* states of the CH_2F and CH_2Cl radicals. Since these species have low ionization potentials, their Rydberg states are low in energy. On the other hand, due to the lone pairs of the halogen substituents, there exist low-lying valence states. Therefore, Rydberg and valence states can strongly interact, and thus a balanced description of both is crucial to the understanding the photoinduced reactions. We have also performed qualitative analysis of the excited states in terms of molecular orbitals, and can explain the changes in the electronic spectra in the $CH_3 \rightarrow CH_2F \rightarrow CH_2Cl$ sequence. The focus of this study is on the vertical electronic excitation spectra. Optimized geometries for the excited states will be reported elsewhere.[29]

In this study, we employ the equation-of-motion coupled-cluster singles and doubles (EOM–CCSD) method, also known as the linear response CC (CCSDLR) model.[30,31] As far as vertical excitation energies are concerned, the EOM–CCSD method can describe singly excited states with remarkable accuracy (0.1–0.3 eV). Unlike multireference models, this accuracy is uniform for the valence and Rydberg states, provided that the excited states are derived predominantly from promotion of a single electron. However, in the case of doublet radicals, the performance of EOM–CCSD may degrade when specific doubly excited valence configurations become important. These configurations involve the

TABLE I. Ground state geometries for CH_2X(X=Cl, F, H) radicals, and CH_2F cation.

	Symm.	r_{CH}, Å	r_{CX}, Å	α_{HCH}	Θ^c	E_{nuc}	E_{tot}
CH_2Cl^a ($X\ ^2B_1$)	C_{2v}	1.076	1.691	124.17	180	45.620 937	−499.007 703
CH_2F^a ($X\ ^2A'$)	C_s	1.079	1.335	124.11	153.11	32.246 535	−138.935 120
CH_2F^a ($X\ ^2B_1$)	C_{2v}	1.076	1.332	127.60	180	32.274 065	−138.934 617
CH_2F^{+a} ($X\ ^1A_1$)	C_{2v}	1.093	1.227	125.77	180	34.192 394	−138.608 190
CH_3^b ($X\ ^2A_2''$)	D_{3h}	1.0767		120	180	9.697 919	

[a]Geometry optimized at CCSD(T)/6-311(++)G(3*df*,3*pd*) level. Pure angular momentum spherical harmonics are used.
[b]MRCI from Ref. 58.
[c]Dihedral HCXH angle.

simultaneous promotion of a spin-α electron from the singly occupied orbital and a spin-β electron into the singly occupied orbital.[32] The natural diagnostics for this situation are provided by (i) the relative weight of doubly excited configurations in the EOM–CCSD wave function; and (ii) the existence of larger spin-contamination. For the excited states reported here, these diagnostics remain uniformly small, which suggests that the EOM–CCSD treatment of these radicals is accurate and reliable.

We also investigate the performance of several computationally inexpensive electronic structure models for these species. We report results for the configuration interaction singles (CIS)[33,34] method; CIS augmented by perturbative corrections, [CIS(D)];[35] and time-dependent density functional theory (TD–DFT)[36] employing the Tamm–Dancoff approximation.[37,38]

The structure of the paper is as follows: Sec. II A outlines computational details, Secs. II B, II C, and II D present the results of the vertical electronic spectra calculations, as well as qualitative analysis of the excited states. Our final remarks and conclusions are given in Sec. III.

II. RESULTS AND DISCUSSION

A. Computational details

Vertical electronic excitation energies for CH_2Cl, CH_2F, and CH_3 are calculated at the geometries summarized in Table I. CH_2Cl and CH_3 are planar in the ground state, which agrees with the experiment.[7,8,23,39,40] Contrary to the experimental results,[15,41,42] CH_2F is found to be nonplanar, with an inversion barrier of 0.014 eV. We shall address this issue, as well as the vibrational spectra of these radicals, elsewhere.[29] In order to estimate how changes from the nonplanar to planar geometry would affect the electronic spectrum, we also report vertical excitation energies at C_{2v} optimized geometry (Table I).

This study employs a 6-311(3+, 3+)G(3df, 3pd) basis set, derived from the polarized split-valence 6-311G(d, p) basis[43,44] by augmenting it by additional sets of polarization and diffuse functions.[45,46] To confirm valence versus Rydberg assignment for low-lying Rydberg states, additional calculations are performed in a 6-311(+, +)G(3df, 3pd) basis set. Pure angular momentum spherical harmonics are used in this study (5 d-functions, 7 f-functions). The third set of diffuse functions is crucial for the correct description of the components of Rydberg *p*- and *d*-states which are perpendicular to the molecular plane. While adding a third set of diffuse functions has no effect on the valence states (including states with high excitation energies), the effect on Rydberg states is very nonuniform. We have found that in the energy range considered the effect does not increase with the excitation energy. Rather, the effect is the greatest for states whose electronic densities exhibit significant changes perpendicular to molecular plane. This is an artifact of atom-centered orbital basis sets: for planar and nearly planar molecules atom-centered basis sets are capable of better spanning of electronic density in the molecular plane than in the perpendicular direction.

As mentioned in the Introduction, in addition to the EOM–CCSD calculations,[30,31] we also report spin-unrestricted CIS,[33,34] CIS(D),[35] and TD–DFT[36] results obtained in a 6-311(3+, 3+)G(3df, 3pd) basis set. TD–DFT calculations employ the Tamm–Dancoff approximation,[37,38] and Becke3–Lee–Yang–Parr (B3LYP) functional with LYP and VWN correlation functionals.[47]

Calculations were performed using the ACES II[48] and Q-Chem[49] *ab initio* programs. Some basis sets used in this work were obtained from the EMSL database.[50]

One of the questions addressed in this study is the valence versus Rydberg character of the excited states. Even though such assignment is not rigorous, it is of great qualitative value for understanding the dynamics of the electronically excited radicals. To achieve a robust assignment, we required that the following three characteristics be consistent: (i) the spherical average of the charge distribution (calculated as an expectation value of the operator R^2) for the ground and excited states (valence states exhibit a smaller increase in electronic density size than Rydberg states); (ii) the effect of removing two sets of diffuse functions from the basis set (valence states are rather insensitive); and (iii) the character of the molecular orbital to which excitation mainly occur (we identify a canonical Hartree–Fock orbital as having predominantly valence character if it has large overlap with one of the MP2 natural orbitals having largest natural populations[51]).

Quantum numbers are assigned to the Rydberg states based on the following considerations: (i) the Rydberg formula (see below);[10] (ii) the symmetry; and (iii) the calculated second moments, i.e., $\langle X^2\rangle$, $\langle Y^2\rangle$, and $\langle Z^2\rangle$, of the charge distribution. (ii) and (iii) are in particular useful for discriminating between different *m* components.

The Rydberg formula is often used to determine the

quantum numbers n and l of Rydberg states:[10]

$$E_{ex} = \mathrm{IP} - \frac{13.61}{(n-\delta)^2}, \quad (1)$$

where E_{ex} is the excitation energy (in eV) of the Rydberg state, IP is the ionization potential (in eV), n is the principal quantum number, and quantum defect δ is an empirical parameter whose role is to account for the difference between the positively charged complex core cation and the bare nucleus in a hydrogenlike atom. Typical values of δ are 0.9–1.2 for s states, 0.3–0.6 for p states, and smaller or equal to 0.1 for d states.[10] We used experimental values for the vertical ionization potentials, i.e., 8.87 eV for CH_2Cl,[52] 9.22 eV for CH_2F,[53] and 9.84 eV for CH_3.[54]

B. CH_2Cl

The leading electronic configuration in the ground state wave function is

$$(1a_1)^2(2a_1)^2(3a_1)^2(1b_1)^2(4a_1)^2(1b_2)^2(5a_1)^2(6a_1)^2(2b_2)^2(7a_1)^2(2b_1)^2(3b_2)^2(3b_1)^1, \quad (2)$$

with the overall symmetry of the electronic wave function being B_1. $1a_1$, $3a_1$, $1b_1$, $4a_1$, and $1b_2$ are $1s$, $2s$, $2p_y$, $2p_z$, and $2p_x$ chlorine's core orbitals, respectively; the $2a_1$ orbital is $1s$ core orbital of carbon. $6a_1$ and $2b_2$ correspond to symmetric and antisymmetric linear combination of two σ_{CH} bonds. $5a_1$ is the $3s$ orbital of chlorine, and $7a_1$ is the C–Cl σ-bonding orbital, σ_{CCl} (the corresponding antibonding orbital, σ^*_{CCl}, is the virtual $11a_1$ orbital). $3b_2$ is $3p_x$ (lone pair) orbital on chlorine. Up to this point, our assignment of the molecular orbitals is identical to that of Li and Francisco.[27] However, we have found that there is a strong interaction between the $3p_y$ lone pair of Cl and the $2p_y$ unpaired electron of C. As a result, two delocalized orbitals, π_{CCl} $(2b_1)$ and π^*_{CCl} $(5b_1)$, are formed. The bonding π_{CCl} orbital is doubly occupied, and the antibonding π^*_{CCl} orbital hosts the unpaired electron. Thus, an additional half-π bond is formed between C and Cl in the CH_2Cl radical.

The $(p-p)$ π additional bonding has been originally suggested by Andrews and Smith in order to explain the shorter bond length and the higher force constant of the C–Cl bond in the CH_2Cl radical (relative to the corresponding saturated compounds).[8] They have also noticed that this type of bonding would result in an anomalous charge distribution: a complete delocalization of the chlorine lone pair and the unpaired electron from carbon would give a -0.5 charge on carbon, and a $+0.5$ charge on chlorine. We have found that the carbon indeed hosts relatively large negative charge (≈ -0.38), whereas chlorine is slightly positively charged ($\approx +0.03$). Even though the exact values for these charges depend on the electronic density used, and on the partial charge definition employed (i.e., Mulliken or Löwdin charges,[55] or natural atomic charges[56]), the overall trend (i.e., a large negative charge on carbon and a small positive one on chlorine) remains unchanged.

Table II contains the vertical transition energies, oscillator strengths, squared electronic transition dipole moments (further on called transition strengths), and the directions of the transition dipole moments. The vertical transition energies from Table II are shown in Fig. 1 [panel (a)]. A molecular orbital picture of the ground state and valence excited states is shown in Fig. 2.

The lowest excited state of CH_2Cl, $1\,^2A_1$, derives from a valence transition from the antibonding π^*_{CCl} orbital to the antibonding σ^*_{CCl} orbital. Therefore, it is possible that this state is bound, but with the CCl bond considerably elongated. The vertical excitation energy is found to be 4.92 eV. This value is 0.31 eV lower than the MRCI result from Ref. 27. The EOM–CCSD value agrees better with the available experimental information, i.e., 4.96–5.02 eV recently determined by Reisler and co-workers.[22] By using the imaging technique, a maximum photofragment yield (Cl and CH_2) was observed around 4.96–5.02 eV. Their results also suggest that the transition dipole moment for this state is perpendicular to the CCl bond.[22] A similar value (5.01 eV) has

TABLE II. Excited states of CH_2Cl radical. EOM–CCSD/6-311(3+,3+)G($3df$,$3pd$), pure angular momentum.

State[a]	E_{ex}, eV	D_{tr}[b]	μ^2_{tr}, a.u.[c]	Transition[d]
$1\,^2A_1(V)$	4.92	0.0051	0.0423 (y)	$\pi^*_{CCl} \rightarrow \sigma^*_{CCl}$
$1\,^2B_2(V)$	5.24			$n^{Cl}_x \rightarrow \pi^*_{CCl}$
$2\,^2A_1(3sR)$	5.54	0.0008	0.0056 (y)	$\pi^*_{CCl} \rightarrow 3s$
$2\,^2B_1(V)$	6.33	0.0711	0.4584 (z)	$\pi_{CCl} \rightarrow \pi^*_{CCl}$
$2\,^2B_2(3p_xR)$	6.34			$\pi^*_{CCl} \rightarrow 3p_x$
$3\,^2B_1(3p_yR)$	6.61	3×10^{-5}	0.0002 (z)	$\pi^*_{CCl} \rightarrow 3p_y$
$3\,^2A_1(3p_zR)$	6.72	0.0083	0.0505 (y)	$\pi^*_{CCl} \rightarrow 3p_z$
$4\,^2A_1(3d_{z^2}R)$	7.15	0.0002	0.0009 (y)	$\pi^*_{CCl} \rightarrow 3d_{z^2}$
$5\,^2A_1(3d_{x^2-y^2}R)$	7.33	0.0089	0.0496 (y)	$\pi^*_{CCl} \rightarrow 3d_{x^2-y^2}$
$3\,^2B_2(3d_{xz}R)$	7.38			$\pi^*_{CCl} \rightarrow 3d_{xz}$
$4\,^2B_1(3d_{yz}R)$	7.45	3×10^{-5}	0.0001 (z)	$\pi^*_{CCl} \rightarrow 3d_{yz}$
$6\,^2A_1(4sR)$	7.47	0.0022	0.0120 (y)	$\pi^*_{CCl} \rightarrow 4s$
$1\,^4A_2(V)$	7.54			$n^{Cl}_x \rightarrow \sigma^*_{CCl}$
$4\,^2B_2(4p_xR)$	7.67			$\pi^*_{CCl} \rightarrow 4p_x$
$5\,^2B_1(4p_yR)$	7.75	0.0027	0.0144 (z)	$\pi^*_{CCl} \rightarrow 4p_y$
$7\,^2A_1(4p_zR)$	7.76	0.0062	0.0326 (y)	$\pi^*_{CCl} \rightarrow 4p_z$
$8\,^2A_1(4d_{z^2}R)$	7.99	0.0051	0.0262 (y)	$\pi^*_{CCl} \rightarrow 4d_{z^2}$
$9\,^2A_1(V)$	8.02	4×10^{-6}	2×10^{-5}(y)	$\sigma_{CCl} \rightarrow \pi^*_{CCl}$
$5\,^2B_2(4d_{xz}R)$	8.07			$\pi^*_{CCl} \rightarrow 4d_{xz}$
$10\,^2A_1(5sR)$	8.09	0.0001	0.0005 (y)	$\pi^*_{CCl} \rightarrow 5s$
$6\,^2B_1(4d_{yz}R)$	8.12	0.0002	0.0011 (z)	$\pi^*_{CCl} \rightarrow 4d_{yz}$
$2\,^4A_2(3sR)$	8.26			$n^{Cl}_x \rightarrow 3s$

[a]For valence states, the spherical average of charge distribution, $\langle R^2 \rangle$, is smaller than or equal to 44 bohr^2. In the ground state, $\langle R^2 \rangle \approx 38$ bohr^2.
[b]Oscillator strength.
[c]Direction of transition dipole is shown in parentheses. The OZ axis is parallel to the CCl bond, and OY axis is perpendicular to the molecular plane.
[d]Half-filled molecular orbital is $\pi^*_{CCl}(5b_1)$ (see Fig. 2).

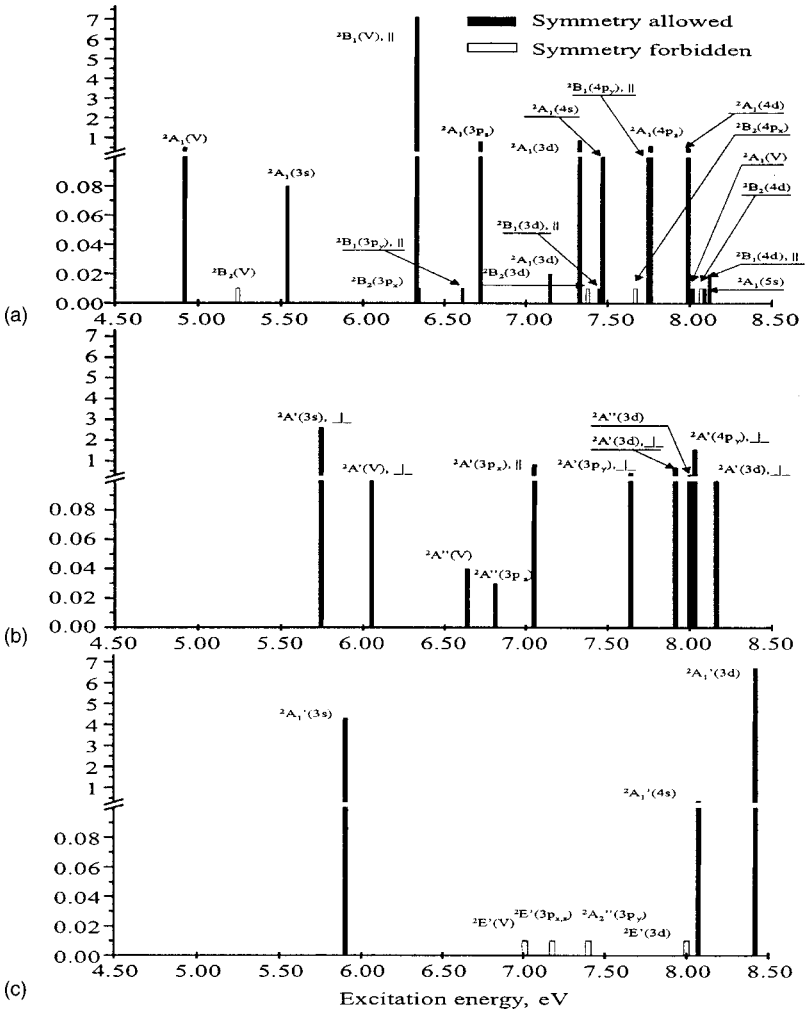

FIG. 1. Vertical excitation energies for CH_2Cl (a), CH_2F (b), and CH_3 (c). Intensities of the transitions are proportional to the oscillator strengths (no Franck–Condon factors are taken into account). Empty bars are used to show positions of forbidden transitions, i.e., those for which oscillator strength is zero due to the symmetry. Transitions are defined as parallel when the transition dipole moment is parallel to the CX bond, and perpendicular otherwise.

been derived by Endo *et al.* from their analysis of the microwave spectrum of CH_2Cl.[23]

The next excited state, $1\,^2B_2$ at 5.24 eV, is optically dark in C_{2v} symmetry. This is also a valence transition, namely, $n_x^{\mathrm{Cl}} \rightarrow \pi^*_{\mathrm{CCl}}$. This dark state is closely followed by a Rydberg $2\,^2A_1$ $(3s)$ state at 5.54 eV. Note that the MRCI study,[27] which employs (i) the full valence active space for the ground and all reported excited states, and (ii) a basis set with no diffuse functions, overestimates the valence character of this transition, and places it 1.4 eV higher in energy. The dominant Rydberg character of this state is confirmed by all three criteria listed in the Sec. II A. In particular, removing two sets of diffuse functions from the basis increases the excitation energy by 0.09 eV. For reference, the biggest observed change in this radical for the valence states is 0.04 eV (detected for the $2\,^2B_1$ and $9\,^2A_1$ states).

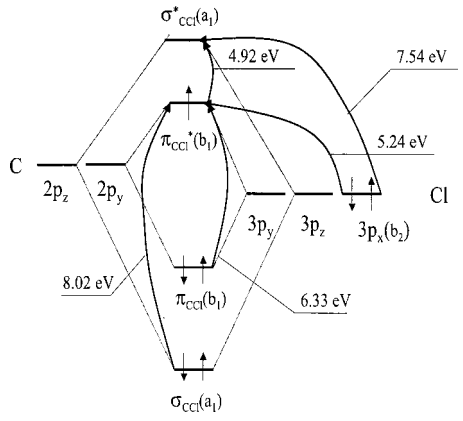

FIG. 2. Molecular orbital picture for the ground and valence excited states of CH_2Cl radical. $7a_1$ orbital is the σ_{CCl} bonding orbital; $2b_1$ orbital is the $(p-p)\pi_{\mathrm{CCl}}$ bonding orbital; $3b_2$ is the $3p_x$ lone pair on Cl atom; $3b_1$ orbital is the singly occupied π-antibonding orbital; and virtual $11a_1$ orbital is the σ^*_{CCl}-antibonding orbital.

The strongest transition in the studied energy interval is to the valence $2\,^2B_1$ state at 6.33 eV. The large value of the transition dipole moment is in agreement with our assignment of this state as $\pi_{\mathrm{CCl}} \rightarrow \pi^*_{\mathrm{CCl}}$ excitation (transitions involving the promotion of an electron from a bonding orbital to the corresponding antibonding orbital are usually the strongest, as shown by Mulliken[57]). This transition was observed experimentally as a broad peak centered around 6.20 eV in the ultraviolet absorption spectrum of CH_2Cl,[18] and it was shown that the transition dipole moment is parallel to the C–Cl bond.[22] The transition is so strong (the absorption cross section is about $1.45\times10^{-17}\,\mathrm{cm}^2\,\mathrm{molecule}^{-1}$), that several other states are likely to be buried under its tails. Note that the EOM–CCSD value for the excitation energy (6.33 eV) is closer to the observed maximum in the absorption

TABLE III. Excitation energies (eV) for CH_2Cl radical. A comparison between EOM–CCSD, CIS, CIS(D), TD–DFT/B3LYP, and MRCI methods.

State	EOM–CCSD[a]	TD–DFT[a]	CIS[a]	CIS(D)[a]	$\langle S^2\rangle_{CIS}$	MRCI[b]	Expt.
$1\,^2A_1(V)$	4.92	4.53	5.72	5.13	0.95	5.23	4.96–5.02 (Refs. 22 and 23)
$1\,^2B_2(V)$	5.24	4.75	6.85	5.51	0.85	5.35	
$2\,^2A_1(3sR)$	5.54	5.00	6.52	5.67	0.93	6.93	
$2\,^2B_1(V)$	6.33	6.04	8.00	6.67	0.90	6.51	6.20 (Ref. 18)
$2\,^2B_2(3p_xR)$	6.34	5.54	7.30	6.39	0.87		
$3\,^2B_1(3p_yR)$	6.61	5.64	7.43	6.55	0.91		6.59 (Ref. 22)
$3\,^2A_1(3p_zR)$	6.72	5.75	7.65	6.80	0.97		
$4\,^2A_1(3d_{z^2}R)$	7.15	5.83	8.13	7.23	0.87		
$5\,^2A_1(3d_{x^2-y^2}R)$	7.33	5.97	8.28	7.36	0.93		
$3\,^2B_2(3d_{xz}R)$	7.38	5.91	8.37	7.37	0.92		
$4\,^2B_1(3d_{yz}R)$	7.45	6.00	8.42	7.44	0.94		
$6\,^2A_1(4sR)$	7.47	6.03	8.43	7.41	0.91		
$1\,^4A_2(V)$	7.54	7.08	7.73	7.63	2.64		
$4\,^2B_2(4p_xR)$	7.67	5.99	8.64	7.59	0.89		
$5\,^2B_1(4p_yR)$	7.75	6.22	8.70	7.65	0.90		
$7\,^2A_1(4p_zR)$	7.76	6.17	8.71	7.74	1.03		
$8\,^2A_1(4d_{z^2}R)$	7.99	6.36	8.97	7.91	0.92		
$9\,^2A_1(V)$	8.02	7.75	8.87	8.47	1.51		
$5\,^2B_2(4d_{xz}R)$	8.07	6.27	9.04	7.97	0.91		
$10\,^2A_1(5sR)$	8.09	6.54	9.05	7.98	0.92		
$6\,^2B_1(4d_{yz})$	8.12	6.63	9.09	8.03	0.94		
$2\,^4A_2(3sR)$	8.26	7.64	8.78	8.28	2.69		

[a]6-311(3+,3+)G($3df$,$3pd$) basis set, pure angular momentum. Geometry is from Table I.
[b]MRCI from Ref. 27. The full valence active space is used for CASSCF reference. Basis set is cc-pVTZ.

spectrum (6.20 eV) than the MRCI value of 6.51 eV.[27]

Except for the very weak $\sigma_{CCl}\rightarrow\pi^*_{CCl}$ transition at 8.02 eV (to the $9\,^2A_1$ state), all other doublet states in this energy interval are Rydberg states. Since all Rydberg states reported here involve excitations of the unpaired electron from the π^*_{CCl} orbital, we expect them to have planar structures with a contracted CCl bond, and a higher C–Cl and out-of-plain vibrational frequencies. Reisler and co-workers[22] have detected a $3p$ Rydberg state at 6.59 eV by $2+1$ REMPI technique. Most likely, this is the $3\,^2B_1$ ($3p_y$) state for which the EOM–CCSD energy is 6.61 eV.

In the energy region examined there are two quartet states, both of A_2 symmetry: the valence ($n_x^{Cl}\rightarrow\sigma^*_{CCl}$) state at 7.54 eV, and the Rydberg ($n_x^{Cl}\rightarrow 3s$) state at 8.26 eV. As expected from qualitative considerations, the corresponding doublet states lie higher in energy (for quartet states, Pauli repulsion keeps the electrons apart, thus resulting in smaller electron–electron repulsion). Note that in closed shell molecules, where any excitation unpairs electrons, the lowest excited state is usually a triplet state. In doublet radicals, however, low-lying states are promotions of the unpaired electron, and, therefore, are doublets. Nevertheless, when excitation energy becomes high enough to involve excitation of ''core'' electrons, quartets have lower energies than the corresponding doublets.

Table III compares the results of CIS, CIS(D), and TD–DFT methods with the EOM–CCSD model, and summarizes the available experimental data. As usual, CIS systematically overestimates the excitation energies by at least 1 eV (up to 1.7 eV for the valence $1\,^2B_2$ and $2\,^2B_1$ states). The seemingly smaller errors for the quartet states are artifacts of the large spin-contamination of these states.

Since the electronic spectrum is rather dense, errors of 1 eV and more could result in a totally incorrect ordering of the excited states, but, since the CIS errors are systematic, the relative order of states has only a few errors.

CIS(D) model represents a systematic improvement: errors against EOM–CCSD are about 0.1 eV or less for most of the states (the maximum error does not exceed ~0.45 eV). Moreover, the double corrections partially restore the correct order of the excited states.

The TD–DFT results are more accurate for valence states than those of CIS: excitation energies are underestimated by 0.3–0.5 eV. However, due to the incorrect asymptotic behavior of the functional used, the errors for

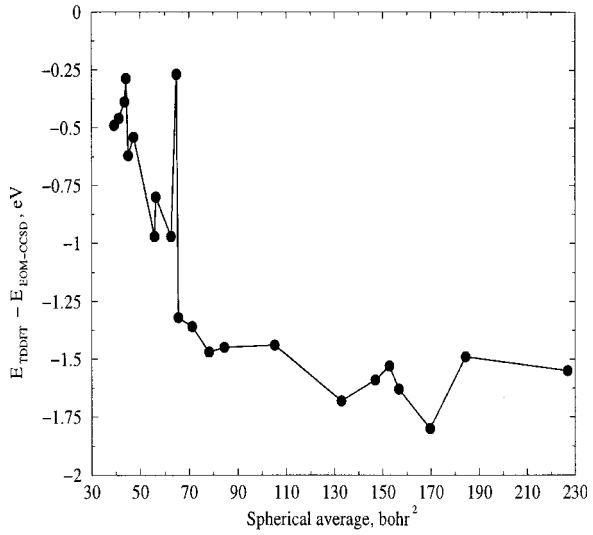

FIG. 3. Errors in the TD–DFT excitation energies vs spherical average of the charge distribution for the CH_2Cl radical.

Rydberg states increase from 0.54 eV for the $3s$ state up to about 1.5–1.7 eV for the higher states. As shown in Fig. 3, the TD–DFT errors are proportional to the size of the electron density.

As explained above, due to a poor basis set selection, the MRCI results[27] overestimate the valence character of the excited states, resulting in errors in the excitation energies of 0.11–1.39 eV.

C. CH_2F

The leading electronic configuration in the ground state wave function is

$$(1a')^2(2a')^2(3a')^2(4a')^2(1a'')^2(5a')^2(6a')^2(2a'')^2(7a')^1, \tag{3}$$

with the overall symmetry of the ground state electronic wave function being A'. $1a'$ and $2a'$ are $1s$ core orbitals on fluorine and carbon, respectively. $6a'$ orbital is the σ_{CF} bond, $2a''$ is the $2p_z$ lone pair orbital on fluorine (perpendicular to the symmetry plane), and $7a'$ is the singly occupied $2p_x$ lone pair on carbon. $3a'$ is the $2s$ orbital on F, $4a'$ and $1a''$ are the symmetric and antisymmetric combinations of the localized σ_{CH} bonds. $5a'$ orbital is the $2p_x$ lone pair on fluorine, which is significantly lowered in energy by partial hybridization with the $2s$ orbital on F. Note that, unlike in CH_2Cl, there is no significant $(p-p)\pi$ bonding between C and F because the large energy gap between the lone pairs on F and the unpaired electron on carbon prevents delocalization. Consequently, there is no anomalous charge distribution in CH_2F (carbon and fluorine host positive and negative charges, respectively), and there is only a minor C–F bond contraction in CH_2F relative to the corresponding saturated compounds.[42]

The absence of additional $(p-p)\pi$ bonding and the lower energies of the fluorine's lone pairs are the two factors that cause the major differences in the electronic spectrum of CH_2F as compared to CH_2Cl. As shown in Table IV and Fig. 1 [panel (b)], (i) the lowest excited state in CH_2F is a Rydberg $2\,^2A'(3s)$ state at 5.74 eV; (ii) in the energy interval studied, there are only two valence states, $3\,^2A'$ at 6.05 eV and $1\,^2A''$ at 6.64 eV.

Figure 4 shows a molecular orbital picture of the ground and excited valence states in CH_2F. The two lowest valence states can be correlated with two lowest valence states of CH_2Cl: in both cases the lowest valence state derives from the promotion of the unpaired electron to the σ^*_{CX} orbital, while the second state derives from the promotion of an electron to the half-filled orbital. However, the different character of orbitals involved, i.e., delocalization in CH_2Cl versus localization in CH_2F, results in a more than 1 eV rise in the excitation energies. The rest of the excited states in this energy interval are Rydberg states deriving from promotions of the unpaired electron. These states are expected to be planar, with a slightly contracted CF bond.

Unlike the CH_2Cl case, the assignment of the Rydberg states is more problematic for CH_2F: the calculated spectrum does not agree well with the one estimated by Eq. (1). Moreover, the calculated second momenta of the charge distribution suggest significant mixing of different angular momentum components, i.e., *ns*, *np*, and *nd* Rydberg states. Therefore, the assignment given in the Table IV is very approximate. A possible reason for the strong coupling (and, therefore, mixing) of the different angular momentum components of Rydberg states may be the relatively large charge separation in the core cation.

Since the barrier between the two C_s minima in the

TABLE IV. Excited states of CH_2F radical. EOM–CCSD/6-311(3+,3+)G($3df$,$3pd$).

State[a]	E_{ex}, eV	D_{tr}[b]	μ^2_{tr}, a.u.[c]	Transition[d]	At C_{2v} geometry[e]
$2\,^2A'(3sR)$	5.74	0.0262	0.1862 (xy)	$2p_x^C \rightarrow 3s$	5.47 (A_1)
$3\,^2A'(V)$	6.05	0.0010	0.0069 (xy)	$2p_x^C \rightarrow \sigma^*_{CF}$	5.76 (A_1)
$1\,^2A''(V)$	6.64	0.0004	0.0022 (z)	$n_z^F \rightarrow 2p_x^C$	6.90 (B_2)
$2\,^2A''(3p_zR)$	6.81	0.0003	0.0015 (z)	$2p_x^C \rightarrow 3p_z$	6.50 (B_2)
$4\,^2A'(3p_xR)$	7.05	0.0084	0.0480 (xy)	$2p_x^C \rightarrow 3p_x$	6.80 (B_1)
$5\,^2A'(3p_yR)$	7.64	0.0044	0.0233 (xy)	$2p_x^C \rightarrow 3p_y$	7.31 (A_1)
$6\,^2A'(3d_{y^2}R)$	7.91	0.0070	0.0362 (xy)	$2p_x^C \rightarrow 3d_{y^2}$	7.62 (A_1)
$3\,^2A''(3d_{zy}R)$	8.00	0.0035	0.0179 (z)	$2p_x^C \rightarrow 3d_{zy}$	7.75 (B_2)
$7\,^2A'(4p_yR)$	8.03	0.0158	0.0802 (xy)	$2p_x^C \rightarrow 4p_y$	7.75 (A_1)
$8\,^2A'(3d_{xy}R)$	8.16	0.0014	0.0068 (xy)	$2p_x^C \rightarrow 3d_{xy}$	7.91 (B_1)

[a]For valence states, the spherical average of charge distribution is smaller than or equal to 29 bohr^2. In the ground state, $\langle R^2\rangle \approx 22$ bohr^2.
[b]Oscillator strength.
[c]Direction of transition dipole is shown in parentheses. The C_s plane is OXY, and the C–F bond is parallel to OY axis. OZ axis is perpendicular to the symmetry plane.
[d]Half-filled molecular orbital is $2p_x^C$ (see Fig. 4).
[e]See Table I.

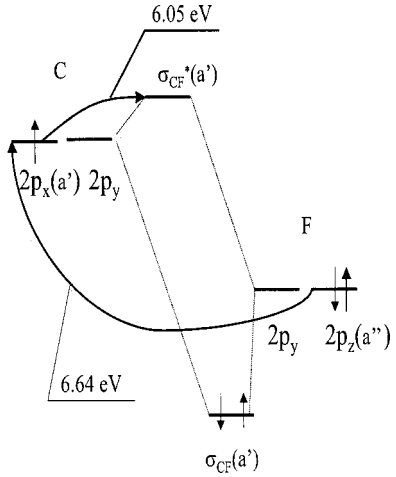

FIG. 4. Molecular orbital picture for the ground and valence excited states of CH_2F radical. $6a'$ is the σ_{CF} bonding orbital; $2a''$ is the $2p_z$ lone pair on F atom; $7a'$ is the carbon *p*-orbital hosting the unpaired electron; and virtual $12a'$ orbital is the σ_{CF}^*-antibonding orbital.

ground state is very small, i.e., 0.014 eV at the CCSD(T) level, it is possible that the zero-point vibrational level is above the barrier. In this case, the radical would behave as effectively planar, which would reconcile the theoretical predictions (C_s structure) with the experimental observations supporting a C_{2v} symmetry.[15,41,42] We shall address this point in a subsequent publication.[29] In order to estimate the possible effect of this pseudo-planar behavior on the electronic spectrum, we also report (Table IV) excitation energies calculated at the C_{2v} optimized geometry (Table I). Note that the difference in excitation energies exceeds the ground state energy difference of 0.014 eV: all excitations energies are lowered by 0.25–0.33 eV (relative to the C_s structure), except for the $1\,^2A''$ state, which is 0.26 eV higher in C_{2v}. This behavior is readily rationalized: all excited states except $1\,^2A''$ involve excitation of the unpaired electron and thus are expected to exhibit a more cationlike (i.e., planar) structure. Therefore, their energies are lower at the planar geometry. In contrast, the $1\,^2A''$ state involves a promotion of an electron from the lone pair on fluorine to a half-filled $2p$ orbital of carbon. This electronic configuration suggests sp^3 hybridization of carbon, and, subsequently, a nonplanar structure. Therefore, the energy of this state is lower for C_s geometry. The important conclusion, however, is that the overall effect does not exceed 0.33 eV.

Some of the Rydberg states of the CH_2F radical have been probed experimentally by Hudgens *et al.*[15] They have reported the 0_0^0 transition energies for the $3p$, $4p$, and $5p$ states of 6.55, 7.85, and 8.34 eV, respectively. The components (i.e., *x*,*y*,*z* components of the *np* states) have not been assigned.[15] This, as well as the poor performance of the Rydberg formula (which has been used to assign the experimentally observed transitions[15]), complicates the comparison with the experimental results. Unfortunately, the calculated transition strengths cannot be used to identify which components of the *np* states were detected, since the experiment involves two-photon transitions.[15] Assuming that the EOM–CCSD errors do not exceed 0.3 eV, the experimentally observed transitions can be assigned as excitations to the $3p_z$ and $4p_y$ states (based on both C_s and C_{2v} vertical excitation energies). We also performed a simple estimation of the adiabatic excitation energies by calculating excited states at the equilibrium geometry of the cation, CH_2F^+ (Table I), as well as estimations of the zero-point energy contributions by using the experimental frequencies.[15] The corresponding excitation energies are 6.53 and 7.79 eV for the $3p_z$ and $4p_y$ states, respectively. Lastly, with zero-point energy corrections, the theoretical 0_0^0 transition energies for the $3p_z$ and $4p_y$ states are 6.62 eV and 7.88 eV, respectively. These numbers are also within 0.3 eV of the experimental values.

The vertical excitation energies for the CH_2F radical calculated by CIS, CIS(D), and TD–DFT are presented in Table V. CIS and CIS(D) perform rather similarly to the CH_2Cl case, the errors being slightly larger. The spin-contamination of the CIS states is smaller and more uniform. That is why the ordering of states by CIS and CIS(D) is almost correct (and, perhaps, also because the spectrum is less dense). The performance of TD–DFT in this case is poor: the errors are not uniform, and gradually increase from 0.4–0.6 eV (for valence states) up to 1.87 eV for the higher Rydberg states. The errors are larger than in the CH_2Cl case because of the increasing Rydberg character in the excited states.

TABLE V. Excitation energies (eV) for CH_2F radical. A comparison between EOM–CCSD, CIS, CIS(D), and TD–DFT/B3LYP methods.[a]

State	EOM–CCSD	TD–DFT	CIS	CIS(D)	$\langle S^2\rangle_{CIS}$	Expt. (E_{00}) (Ref. 15)
$2\,^2A'(3sR)$	5.74	4.97	6.76	5.82	0.78	
$3\,^2A'(V)$	6.05	5.42	7.05	6.19	0.79	
$1\,^2A''(V)$	6.64	6.21	8.05	6.98	0.81	
$2\,^2A''(3p_zR)$	6.81	5.72	7.82	6.80	0.78	6.55
$4\,^2A'(3p_xR)$	7.05	5.86	8.06	7.06	0.79	
$5\,^2A'(3p_yR)$	7.64	6.00	8.77	7.66	0.79	
$6\,^2A'(3d_{y^2}R)$	7.91	6.11	9.01	7.84	0.79	
$3\,^2A''(3d_{zy}R)$	8.00	6.13	9.15	7.93	0.79	
$7\,^2A'(4p_yR)$	8.03	6.30	9.13	7.92	0.78	7.85
$8\,^2A'(3d_{xy}R)$	8.16	6.31	9.32	8.06	0.79	

[a]6-311(3+,3+)G($3df$,$3pd$) basis set, pure angular momentum. Geometry is from Table I.

TABLE VI. Excited states of CH_3 radical. EOM–CCSD/6-311(3+,3+)G($3df$,$3pd$), pure angular momentum.

State[a]	E_{ex}, eV	D_{tr}[b]	μ_{tr}^2, a.u.[c]	Transition[d]
$1\,^2A_1'(3sR)$	5.90	0.0431	0.2983 (y)	$2p_y^C \rightarrow 3s$
$1\,^2E'(V)$	7.01			$\sigma_{CH} \rightarrow 2p_y^C$
$2\,^2E'(3p_{x,z}R)$	7.18			$2p_y^C \rightarrow 3p_x, 3p_z$
$2\,^2A_2''(3p_yR)$	7.40			$2p_y^C \rightarrow 3p_y$
$3\,^2E'(3d_{yz,xy}R)$	8.00			$2p_y^C \rightarrow 3d_{yz}, 3d_{xy}$
$2\,^2A_1'(4sR)$	8.07	0.0038	0.0193 (y)	$2p_y^C \rightarrow 4s$
$3\,^2A_1'(3d_{xz}R)$	8.42	0.0670	0.3250 (y)	$2p_y^C \rightarrow 3d_{xz}$
$4\,^2E'(4p_{x,z}R)$	8.53			$2p_y^C \rightarrow 4p_x, 4p_z$
$3\,^2A_2''(4p_yR)$	8.61			$2p_y^C \rightarrow 4p_y$

[a]For valence states, the spherical average of charge distribution is smaller than or equal to 12 bohr^2. $\langle R^2 \rangle$ for the ground state is 10 bohr^2.
[b]Oscillator strength.
[c]Direction of transition dipole is shown in parentheses. The CH_3 molecule is in OXZ plane.
[d]Half-filled molecular orbital is $2p_y^C$ (see Fig. 5).

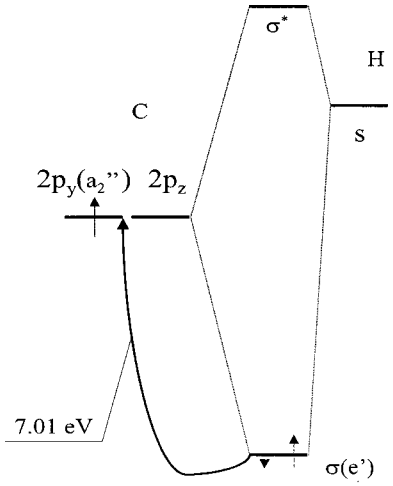

FIG. 5. Molecular orbital picture for the ground and valence excited states of CH_3 radical. 1 and $2e'$ are the doubly degenerate combination of the localized C–H bonds; and $1a_2''$ is carbon's p-orbital hosting the unpaired electron.

D. Comparisons of the excited states in the $CH_3 \rightarrow CH_2F \rightarrow CH_2Cl$ sequence

In order to address the issue of the effect of the halogen atoms on the electronic spectrum, we compare the character of the excited states in the $CH_3 \rightarrow CH_2F \rightarrow CH_2Cl$ sequence.

The electronic configuration of the ground state of the CH_3 radical is

$$(1a_1')^2(2a_1')^2(1e')^4(1a_2'')^1. \tag{4}$$

The electronic symmetry of the ground state is A_2''. $1a_1'$ is the carbon core orbital, $2a_1'$ and $1e'$ are totally symmetric and doubly degenerate combinations of the localized σ_{CH} bonds, respectively, and $1a_2''$ is the singly occupied $2p_y$ orbital.

Table VI and Fig. 1 [panel (c)] show vertical excitation energies for CH_3. The molecular orbital picture of the ground and a valence excited states is shown in Fig. 5.

Due to the absence of the lone pairs of halogen, the lowest valence state in CH_3 involves excitation from a bonding σ_{CH} orbital to a half-occupied p_y orbital on carbon, located at 7.01 eV. The rest of the states in this energy interval are Rydberg states involving promotion of the unpaired electron.

Note that the lowest Rydberg state in all three radicals derives from a promotion of the unpaired electron to a $3s$ Rydberg orbital. The excitation energies for this Rydberg state appear to be surprisingly insensitive to the core cation nature (5.90 eV in CH_3, 5.74 eV in CH_2F, and 5.54 eV in CH_2Cl). The similar result holds for the $3p$ Rydberg states as well: the excitation energies for all three radicals lie within 1 eV, the differences being smaller between CH_3 and CH_2F (about 0.4 eV). Therefore, the nature and even the excitation energies for the low-lying Rydberg states are similar in all three radicals. The transition strengths, however, are very different due to symmetry imposed selection rules, i.e., the $B_1 \rightarrow B_2$ transition is forbidden in C_{2v}, and the $A_2'' \rightarrow A_2'$, $A_2'' \rightarrow A_2''$, $A_2'' \rightarrow E'$, and $A_2'' \rightarrow A_1''$ ones are forbidden in D_{3h} symmetry.

The valence states, however, are very different. The number of low-lying valence states increases as we move from CH_3 to CH_2F, and then to CH_2Cl. The key factors determining the character and excitation energies of the valence states are the presence of the lone pairs on halogen, and how strongly they are bound to the halogen. As far as valence states in CH_2F and CH_2Cl are concerned, the nature of the two lowest valence states is very similar, however, the lowest valence state in CH_2F lies more than 1 eV above the lowest valence state in CH_2Cl.

TABLE VII. Excitation energies (eV) for CH_3 radical. A comparison between EOM–CCSD, CIS, CIS(D), TD–DFT/B3LYP, and MRCI methods.[a]

State	EOM-CCSD	TD-DFT	CIS	CIS(D)	$\langle S^2 \rangle_{CIS}$	MRCI (Ref. 11)	Expt. (E_{00})
$1\,^2A_1'(3sR)$	5.90	5.20	6.55	6.02	0.76	5.86	5.73 (Ref. 12)
$1\,^2E'(V)$	7.01	6.87	7.95	7.31	0.78	7.13	
$2\,^2E'(3p_{x,z}R)$	7.18	6.06	7.77	7.18	0.77	6.95	
$2\,^2A_2''(3p_yR)$	7.40	6.17	7.95	7.46	0.77	7.37	7.44 (Ref. 13)
$3\,^2E'(3d_{yz,xy}R)$	8.00	6.40	8.72	8.05	0.76	8.03	
$2\,^2A_1'(4sR)$	8.07	6.27	8.75	8.07	0.76	8.10	
$3\,^2A_1'(3d_{xz}R)$	8.42	6.64	9.07	8.45	0.76	8.36	8.2 (Ref. 12)
$4\,^2E'(4p_{x,z}R)$	8.53	6.62	9.21	8.47	0.76		
$3\,^2A_2''(4p_yR)$	8.61	6.62	9.26	8.54	0.77		8.66 (Ref. 14)

[a]6-311(3+,3+)G($3df$,$3pd$) basis set, pure angular momentum. Geometry is from Table I.

Table VII presents the excitation energies calculated by the CIS, CIS(D), and TD–DFT methods. CIS overestimates excitation energies by about 0.5–0.7 eV, except the valence state, for which the error is 0.94 eV. CIS(D) performs very well for the Rydberg states: it gives an error of 0.12 eV for the first ($3s$) state, and then the errors become less than 0.1 eV. The excitation energy to the valence $1\,^2E'$ state is overestimated by 0.3 eV. Similarly to CH_2Cl and CH_2F, the TD–DFT errors in excitation energies for the Rydberg states are large, i.e., 0.7–2 eV. Moreover, the TD–DFT ordering of states is erroneous, despite the fact that the spacing between individual states is relatively large for this radical. The MRCI excitation energies, calculated by Mebel and Lin[11] (see Table VII), differ from the EOM–CCSD excitation energies by no more than 0.23 eV, with the difference for four states out of the seven considered being smaller than 0.05 eV.

III. CONCLUSIONS

In this work, we report the vertical electronic excitation energies for CH_2Cl, CH_2F, and CH_3 radicals, and present a qualitative molecular orbital picture for the ground and excited states. The key factors determining the character of the ground state and valence excited states are (i) the presence of lone pairs on halogen and (ii) how strongly these lone pairs are bound to the halogen. The small energy gap between the unpaired electron of carbon and the lone pair of chlorine results in an additional $(p-p)-\pi$ bonding in CH_2Cl. This explains why the CCl bond is shorter and stronger in CH_2Cl as compared to the saturated compound. In contrast, there is no significant electron delocalization, and, therefore, additional bonding in CH_2F.

The energies and the character of the valence excited states are also determined by the energies of halogen lone pairs. As expected, the number of low-lying valence states increases in $CH_3 \rightarrow CH_2F \rightarrow CH_2Cl$ sequence. In CH_2F and CH_2Cl the nature of the two lowest valence states is similar, but the lowest valence state in CH_2F lies more than 1 eV above the lowest valence state in CH_2Cl. The low-lying Rydberg states appear to be similar in all three radicals, i.e., the excitation energies for $3s$, $3p$, and $4s$ states are found to be rather insensitive to the core cation nature. The transition strengths, however, are very different due to symmetry selection rules. As a general trend, the Rydberg excited states in CH_2F are more similar to those in CH_3, rather than to those in CH_2Cl.

We have also investigated the performance of less expensive electronic structure models for these radicals. The major conclusion is that TD–DFT/B3LYP[47] yields rather large and nonsystematic errors (due to the incorrect asymptotic behavior of the functional employed). The performance of CIS is more uniform, and, even though the errors are rather large (>1 eV), the accuracy of CIS is approximately the same for all three radicals, and the ordering of states is reproduced better than by TD–DFT. CIS(D) model presents a systematic improvement over CIS.

The atmospheric implications concern the interesting question posed by Li and Francisco:[27] do these radicals absorb significantly solar light at the wavelengths available at altitudes around 30 km, i.e., where there is a maximum in ozone abundance.[1] At this altitude, significant actinic fluxes are available at the wavelengths >280 nm ($E<4.43$ eV). The vertical excitation for the lowest excited state in CH_2Cl is about 0.5 eV higher. Nevertheless, a definite conclusion about the importance of the photoabsorption at these wavelengths can be drawn only when Franck–Condon factors are taken into account. We shall address this question in a subsequent publication.[29] The actinic fluxes available at 190–230 nm (5.34–6.53 eV) are two orders of magnitude lower, but still considerable. Therefore, one may expect a considerable absorption by CH_2Cl, since its strongest electronic transition has been found to be at 6.20–6.33 eV. The strongest transition in CH_2F, i.e., to the $2\,^2A'$ state, also occurs in this interval (at 5.74 eV).

ACKNOWLEDGMENTS

One of the authors (A.I.K.) acknowledges support from the National Science Foundation CAREER Award (Grant No. CHE-0094116), the Camille and Henry Dreyfus New Faculty Awards Program, and the Donors of the Petroleum Research Fund, administered by the American Chemical Society. The authors wish to thank Professor J.F. Stanton for giving access to ACES II *ab initio* program,[48] and for valuable help in setting up some calculations and resolving some problems. The authors are also grateful to Professor H. Reisler and her group for stimulating discussions, and for sharing their results prior to publication.

[1] B. J. Finlayson-Pitts and J. N. Pitts, *Chemistry of the Upper and Lower Atmosphere: Theory, Experiments, and Applications* (Academic, New York, 1999).
[2] J. S. Francisco and M. M. Maricq, Atmospheric photochemistry of alternative halocarbons, in *Advances in Photochemistry* (Wiley, New York, 1995), Vol. 20, pp. 79–163.
[3] M. E. Jacox, J. Phys. Chem. Ref. Data, 1 (1994), Monograph No. 3.
[4] K. Morokuma, L. Pedersen, and M. Karplus, J. Chem. Phys. **48**, 4801 (1968).
[5] T. G. Carver and L. Andrews, J. Chem. Phys. **50**, 4235 (1969).
[6] T. G. Carver and L. Andrews, J. Chem. Phys. **50**, 4223 (1969).
[7] M. E. Jacox and D. E. Milligan, J. Chem. Phys. **53**, 2688 (1970).
[8] L. Andrews and D. W. Smith, J. Chem. Phys. **53**, 2956 (1970).
[9] D. W. Smith and L. Andrews, J. Chem. Phys. **58**, 5222 (1970).
[10] G. Herzberg, *Molecular Spectroscopy and Molecular Structure; Electronic Spectra and Electronic Structure of Polyatomic Molecules* (van Nostrand Reinhold, New York, 1966), Vol. III.
[11] A. M. Mebel and S.-H. Lin, Chem. Phys. **215**, 329 (1997).
[12] G. Herzberg and J. Shoosmith, Can. J. Phys. **34**, 523 (1956).
[13] J. W. Hudgens, T. G. DiGiuseppe, and M. C. Lin, J. Chem. Phys. **79**, 571 (1983).
[14] J. F. Black and I. Powis, J. Chem. Phys. **89**, 3986 (1988).
[15] J. W. Hudgens, C. S. Dulcey, and G. R. Long, J. Chem. Phys. **87**, 4546 (1987).
[16] G. R. Long and J. W. Hudgens, J. Phys. Chem. **91**, 5870 (1987).
[17] B. P. Tsai, R. D. Johnson III, and J. W. Hudgens, J. Phys. Chem. **93**, 5334 (1989).
[18] P. B. Roussel, P. D. Lightfoot, F. Caraip, V. Catoire, R. Lesclaux, and W. Forst, J. Chem. Soc., Faraday Trans. **87**, 2367 (1991).
[19] O. J. Nielsen, J. Munk, G. Locke, and T. J. Wallington, J. Phys. Chem. **95**, 8714 (1991).
[20] E. Villenave and R. Lesclaux, Chem. Phys. Lett. **236**, 376 (1995).
[21] C. K. Chong, X. Zheng, and D. L. Phillips, Chem. Phys. Lett. **328**, 113 (2000).
[22] V. Dribinski, A. Demyanenko, A. Potter, and H. Reisler, J. Chem. Phys. **115**, 7474 (2001), preceding paper.
[23] Y. Endo, S. Saito, and E. Hirota, Can. J. Phys. **62**, 1347 (1984).

[24] D. V. Dearden, J. W. Hudgens, R. D. Johnson III, B. P. Tsai, and S. A. Kafafi, J. Phys. Chem. **96**, 585 (1992).
[25] J. W. Hudgens, R. D. Johnson III, and B. P. Tsai, J. Chem. Phys. **98**, 1925 (1993).
[26] S. A. Kafafi and J. W. Hudgens, J. Phys. Chem. **93**, 3474 (1989).
[27] Y. Li and J. S. Francisco, J. Chem. Phys. **114**, 2879 (2001).
[28] Z. Li and J. S. Francisco, J. Chem. Phys. **110**, 817 (1999).
[29] S. V. Levchenko and A. I. Krylov (in preparation).
[30] H. Koch, H. Jørgen, Aa. Jensen, and P. Jørgensen, J. Chem. Phys. **93**, 3345 (1990).
[31] J. F. Stanton and R. J. Bartlett, J. Chem. Phys. **98**, 7029 (1993).
[32] D. Maurice and M. Head-Gordon, J. Phys. Chem. **100**, 6131 (1996).
[33] J. A. Pople, Trans. Faraday Soc. **49**, 1375 (1953).
[34] J. B. Foresman, M. Head-Gordon, J. A. Pople, and M. J. Frisch, J. Phys. Chem. **96**, 135 (1992).
[35] M. Head-Gordon, R. J. Rico, M. Oumi, and T. J. Lee, Chem. Phys. Lett. **219**, 21 (1994).
[36] S. Hirata and M. Head-Gordon, Chem. Phys. Lett. **314**, 291 (1999).
[37] I. Tamm, J. Phys. (Moscow) **9**, 449 (1945).
[38] S. M. Dancoff, Phys. Rev. **78**, 382 (1950).
[39] J. P. Michaut and J. Roncin, Chem. Phys. Lett. **12**, 95 (1971).
[40] T. J. Sears, F. Temps, H. Gg. Wagner, and M. Wolf, J. Mol. Spectrosc. **168**, 136 (1994).
[41] J. A. Mucha, D. A. Jennings, K. M. Evenson, and J. T. Hougen, J. Mol. Spectrosc. **68**, 122 (1977).
[42] Y. Endo, C. Yamada, S. Saito, and E. Hirota, J. Phys. Chem. **79**, 1605 (1983).
[43] R. Krishnan, J. S. Binkley, R. Seeger, and J. A. Pople, J. Chem. Phys. **72**, 650 (1980).
[44] A. D. McLean and G. S. Chandler, J. Chem. Phys. **72**, 5639 (1980).
[45] M. J. Frisch, J. A. Pople, and J. S. Binkley, J. Chem. Phys. **80**, 3265 (1984).
[46] T. Clark, J. Chandrasekhar, and P. V. R. Schleyer, J. Comput. Chem. **4**, 294 (1983).
[47] P. J. Stephens, F. J. Devlin, C. F. Chabalowski, and M. J. Frisch, J. Phys. Chem. **98**, 11623 (1994).
[48] J. F. Stanton, J. Gauss, J. D. Watts, W. J. Lauderdale, and R. J. Bartlett, ACES II, 1993. The package also contains modified versions of the MOLECULE Gaussian integral program of J. Almlöf and P. R. Taylor, the ABACUS integral derivative program written by T. U. Helgaker, H. J. Aa. Jensen, P. Jørgensen, and P. R. Taylor, and the PROPS property evaluation integral code of P. R. Taylor.
[49] J. Kong, C. A. White, A. I. Krylov *et al.*, J. Comput. Chem. **21**, 1532 (2000).
[50] Basis sets were obtained from the Extensible Computational Chemistry Environment Basis Set Database, Version, as developed and distributed by the Molecular Science Computing Facility, Environmental and Molecular Sciences Laboratory which is part of the Pacific Northwest Laboratory, P.O. Box 999, Richland, WA 99352, USA, and funded by the U.S. Department of Energy. The Pacific Northwest Laboratory is a multi-program laboratory operated by Battelle Memorial Institute for the U.S. Department of Energy under Contract No. DE-AC06-76RLO 1830. Contact David Feller or Karen Schuchardt for further information.
[51] H. J. Aa. Jensen, P. Jørgensen, H. Ågren, and J. Olsen, J. Chem. Phys. **88**, 3834 (1988).
[52] L. Andrews, J. M. Dyke, N. Jonathan, N. Keddar, and A. Morris, J. Am. Chem. Soc. **106**, 299 (1984).
[53] L. Andrews, J. M. Dyke, N. Jonathan, N. Keddar, A. Morris, and A. Ridha, J. Phys. Chem. **88**, 2364 (1984).
[54] J. Dyke, N. Jonathan, E. Lee, and A. Morris, J. Chem. Soc., Faraday Trans. 2 **72**, 1385 (1976).
[55] A. Szabo and N. S. Ostlund, *Modern Quantum Chemistry: Introduction to Advanced Electronic Structure Theory* (McGraw-Hill, New York, 1989).
[56] A. E. Reed, L. A. Curtiss, and F. Weinhold, Chem. Rev. **88**, 899 (1988).
[57] R. S. Mulliken, J. Chem. Phys. **7**, 20 (1939).
[58] P. Botschwina, E. Schick, and M. Horn, J. Chem. Phys. **98**, 9215 (1993).